

# Modeling and Simulation of Crater dimension in Electrical Discharge Machining

Mr. Nishant Mishra<sup>1</sup>, Mr. Atul Chakrawarti<sup>2</sup>

<sup>1</sup> M.Tech Student, Department of Mechanical Engineering,SSIPMT Raipur

<sup>2</sup> Associate Professor, Department of Mechanical Engineering,SSIPMT Raipur

\*\*\*

**Abstract** - A comprehensive model of electrical discharge machining has been used for simulate the crater size during the process for materials Aluminum, Brass and die steel D2. It is very difficult by theoretically to analysis temperature distribution in whole work -piece because of its complexity process and a single discharge is occurs very short time.

A novel model proposed with realistic condition such as plasma radius , Gaussian heat flux and temperature dependent properties and this model use software ABAQUS 6.2 In this work piece crater diameter and depth is predicted on the basis of simulation. FEM model show the variation of crater size (temperature distribution) with variation in input parameter. In model, increasing discharge energy causes crater size increase means MRR and surface roughness increases. In this model, simulation show better result with experimental result and error is taken under consideration like 13 to 20% which is better result in present research scenario.

**Key Words:** Electrical Discharge Machining, FEM model, ABAQUS 6.2, Crater Size, MRR, Surface Roughness.

## 1. INTRODUCTION

Electrical discharge machining is a most used non-traditional machining processing which all thermal energy produced by spark is utilize for remove the material from the work piece .In this EDM process the work piece as anode and tool as cathode is separated by small gap ,this gap is known as spark gap . The work piece and tool are sinking in dielectric medium. Initially dielectric medium is work as insulated medium .the electric power is supply between the gap of tool and work piece when intensity of power supply is greater than intensity of dielectric it cause breakdowns to create plasma channel comprise of electron and positive ion between the tool and work piece. These electrons and ions are accelerated by electrical field after they affect the high velocity electrodes. In localized heating, it causes the removal of materials by melting and evaporation on high temperature anodic and cathodes surfaces of a very small area. But molten material is not flushes completely into a realistic condition, and some of the molten material is still present in the work piece that solidified and reworked the work piece. It causes HAZ due to high temperature gradient.

Fig.1 show schematic diagram of EDM, radius of plasma is maximum at anode compare cathode. Hence maximum material is remove from anode surface.

## 1.1 Electrical Discharge Machining

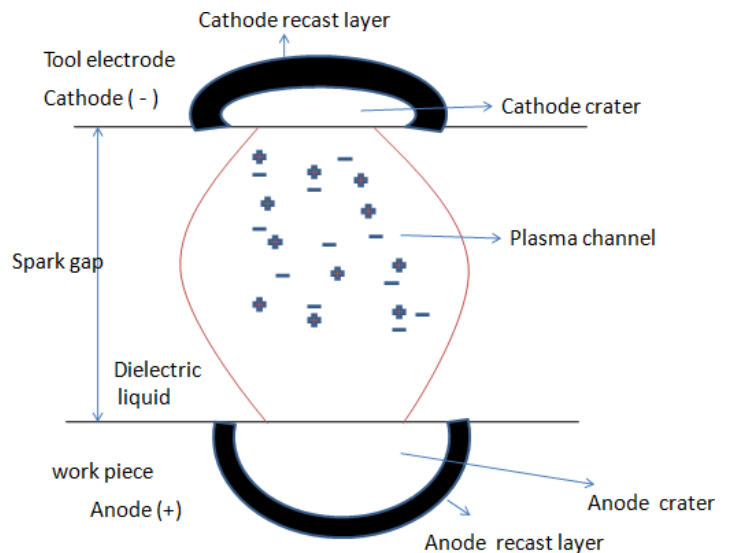


Fig.-1: Schematic of EDM

## 1.2 Characteristics of EDM

The capacity to work difficult equipment is a major benefit because most instruments and molds are produced of difficult components to enhance life. Recent innovations in cutting instruments and high-speed machining procedures allow for the machining of harder components than previously, but EDM stays the only method accessible for machining a large range of difficult components (e.g. carbides).

The work piece gets almost no mechanical stresses because of an EDM procedure relying on a heat concept. This makes it possible to machine very tiny and brittle constructions. It should be noted that the EDM process produces tiny mechanical, power and magnet forces and that wiping and hydraulic forces can become as large as they have

been described for certain working-piece structures. However, the procedures for mechanical extraction do not have big cutting forces.

## 2. FINITE ELEMENT METHOD

This chapter recommends a final component system for the EDM simulation which considers important system elements such as a temperature-dependent materials characteristics, Gaussian thermal flow and varying channels radius, cathodes power percentage and plasma effectiveness. Due to these significant elements, this system can provide a more accurate forecast of the crater profile. The publishers expanded a cathode profile forecasting system to a multi-function situation for the simulation of the texture of the ground produced during the EDM phase during a single release. A method to finite elements can provide a stronger forecast for surface texture. This is because a numerical strategy enables simulation of the complicated thermal stream circumstances that arise from various bubbles simultaneously during the EDM phase. The writers thus strive to create a FEM system which enables accurate forecast of the crater shape of a spark simulation. This distinctive spark system will develop a various system of funneling for the prediction of ground deformation as a potential research.

### 2.1 METHODOLOGY

#### 2.1.1 Electrical-thermal model of single discharge-spark EDM process

At the plasma generated while the job surface is heated, the EDM release can be modeled. Researchers used the device heat source, as previously stated, in thermal EDM modeling with a uniform heat stream or point heat source model. However, these are simple assumptions and do not correspond to the real EDM method. In reality, Kojima et al. and Descoedres et al. [9] have finished contemporary experimental findings by using spectroscopic methods, exposing the non-uniform but mildly comparable temperature distribution of the plasma channel inside the Gaussian model because the pressure at the middle of the plasma chamber is maximal. The thermal flow with Gaussian flow is more essential because the thermal flow in Plasma EDM can be characterized more reliably and in a more sensible way by the suitable system variables that control the release power. In addition, the real structure is closer to that of a random spark than Gaussian. It is the ideal case for the modeling, under appropriate boundary conditions, of a single spark of Gaussian distributed heat stream, in the light of the an axisymmetric nature of the analytical domain. The following parts address the information needed for a single discharge FEM simulation.

#### 2.1.2 Assumptions

1. The material volume removed per discharge, compared with the volume of piece and instrument electrodes, is so small that both the work-piece and the tool are regarded as semi - inestimable organisms.
2. Axisymmetrical for r - z plane is considered for the investigated domain for thermal analysis.
3. Each pulse discharge duration (on-time + off-time) is equal to just a single spark during every pulse.
4. The rest are used both to wear and to dissipate through convections and radiations throughout the dielectric mediums, and only the constant part of Sparks - thermal energy transmit into the work-piece. That assumption is more discussed in section ' ' Energy - sharing gaps ' ' and later at the end of section ' ' Effects of modeling assumptions on the precision of results and comparison with other approvals ' '
5. Conduction and convection are considered the major mode for heat transfer to the spark channel into the work piece surfaces as it is negligible to contribute to other mechanisms like radiation.
6. The work piece is supposed to be homogeneous and isotropic, even as its thermal - physical properties such as a thermal conductivity, density and specific heat due to high temperature gradient during release are regarded as temperature - dependent.
7. The die-electric rush after the collapse of the plasma canal supposes all of the material which temperature exceeds a melting point temperature. In other words, to the base of the crater cavity created at the end of each release no deposition of the recast layer is produced.

## 3. MODELING AND BOUNDARY CONDITION

### 3.1 Modeling Condition

To simulate the die sinking EDM of the die steel D2, aluminium and Brass , a 3-D FEM was used, Because stochastic discharge place and time / space dependent, the ABAQUS / standard was selected for the simulation. In order to accommodate enough electric discharges and show the stochastic nature, the model dimensions were 1500  $\mu\text{m}$  \* 1500  $\mu\text{m}$  \* 400  $\mu\text{m}$ . The finest mesh is 0.5 $\mu\text{m}$  and element type is coupled temperature displacement, it was installed on the working piece surface where the heat flux was applied

and a high resolution was provided for spatial convergence. This model can be shown by fig 2. In this analysis, the temperature field and the thermal damage were calculated using a heat transfer analysis. Physical modeling of machining or crater formation can be understood by fig 3 below.

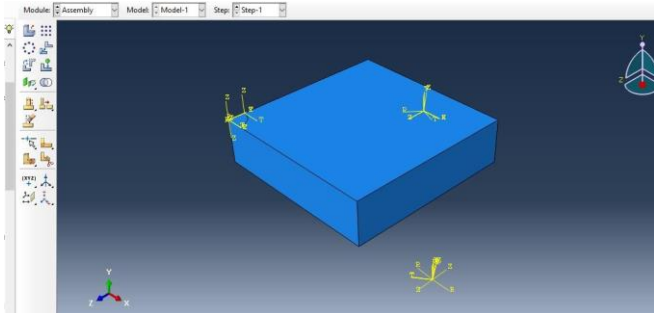


Fig.-2: Modeling Condition

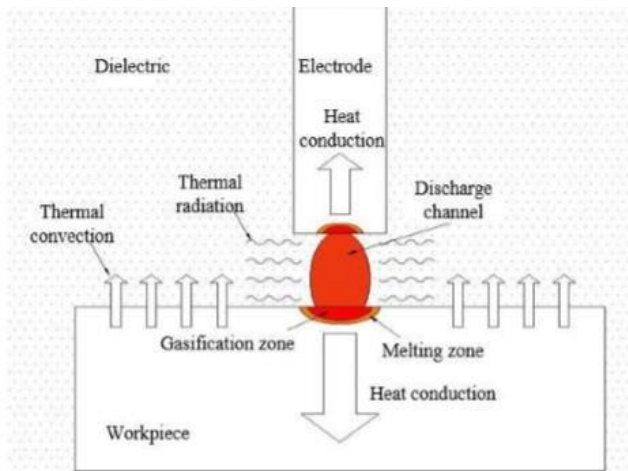


Fig.-3: Physical model of EDM

### 3.2 Boundary Condition

#### 3.2.1 Governing Equation

The regulating equation of the single function setback is the cylindrical co-ordinates Fourier's thermal conductivity equations, as follows:

$$r \frac{\partial T}{\partial r} + \frac{\partial^2 T}{\partial r^2} = \frac{1}{\alpha} \frac{\partial T}{\partial t} \quad \dots\dots\dots (1)$$

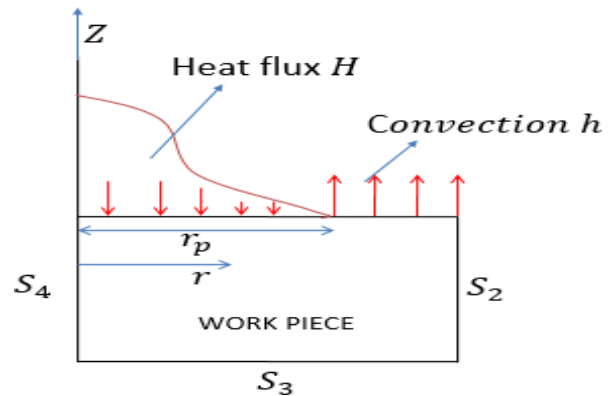


Fig.-4: Condition of distributed heat flux applied

S2, S3 and S4 are surface which are insulated

The boundary conditions are

$$-K \frac{\partial T(0, r, t)}{\partial z} = \begin{cases} H(r, t) & 0 < r < r_p(t) \\ \Delta(T - T_0) & r > r_p(t) \end{cases} \quad \dots\dots (2)$$

$$\frac{\partial T}{\partial R} = 0 \quad \text{at } r=r_p \quad \dots\dots\dots(3)$$

$$\frac{\partial T}{\partial r} = 0 \quad \text{at } r=Z \quad \dots\dots\dots(4)$$

The initial condition is

$$T(r, Z, 0) = T_r \quad \dots\dots\dots(5)$$

where,

r and Z are radius and depth of cylindrical coordinates;

T is a temperature;

T<sub>r</sub> show room temperature;

α show diffusivity of material;

K is a thermal conductivity;

Δ is the heat transfers coefficient,

r<sub>p</sub> is radius of plasma and

q<sub>0</sub> is a heat flux.

The methodical solutions of Equation (1) with assumption such as constant thermal physicals properties, predetermined plasma

radius and identical distributed heat flux, has been found into. The forecast of the models do not match to experimental findings. Some test remarks have lead to questions concerning to the consistent distributed heat flow and constant plasma radius hypothesis. A model used in this lessons replace heat source to a heat source expanding.

### 3.3 General Properties of Material

**Table -1:** General Property Of Materials

MATERIAL	TEM. K	SPECIFIC HEAT J / kg <sup>0</sup> C	CONDUCTIVITY W / m <sup>0</sup> C	DENSITY kg / m <sup>3</sup>	ELASTICITY N/m <sup>2</sup>
ALUMINIUM	298	242	237	2700	70E9
BRASS	298	162	111	8600	97E9
DIE STEEL D2	298	461	20	7700	210E9

### 4. SIMULATION AND RESULT

Table 2 present input parameters and condition for the simulation condition like discharge on time, discharge current and gap voltage.

**Table-2:** Simulation Condition

t <sub>on</sub> μs	I amp	VOLTAGE V	DISCHARGE ENERGY mJ	PFE
14	5	50	3.5	0.8211
20	8	50	8	0.8883
25	10	50	12.5	0.9331

The effect of various input parameters in simulated craters dimension are investigated by parametric analysis. A number of FEM simulations is done by the parameters variations. Analysis of plasma flush efficiency can be calculated by equation 23155. This shows that the flush efficiency is small with small current and large pulse times, so the resolidification is high. In contrast, the flushing efficiency is maximal to high current and low pulse in time combinations, indicating a much lower resolidification level. In this model temperature dependent properties are used like thermal conductivity, density and specific heat. The value of heat

convection varies according to authors for die sinking liquid, but we consider the value of heat convection is 8000 W/m<sup>2</sup>.

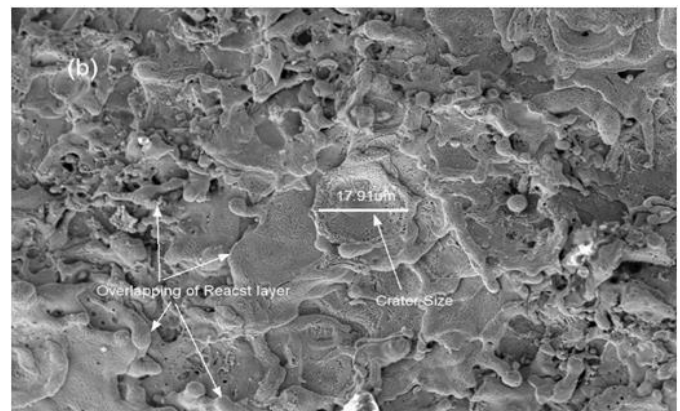


**Fig-5:** Experimental result (aluminum) at I-5A t<sub>on</sub>-14μs, Gap volt-50V

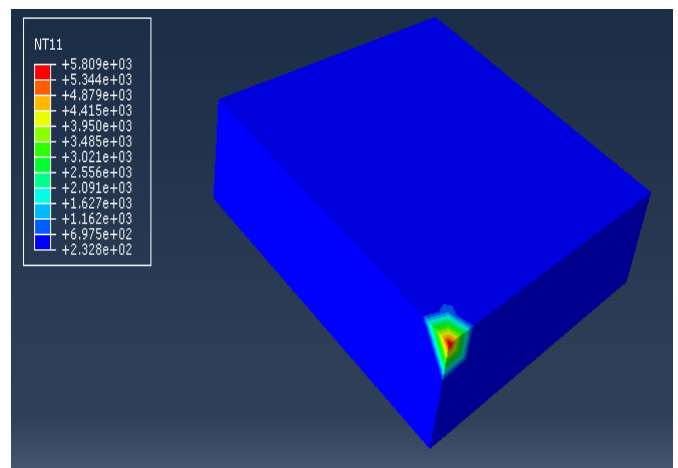


**Fig-6:** Simulation result (aluminum) at I-5A, t<sub>on</sub> -14μs, Gap volt-50V

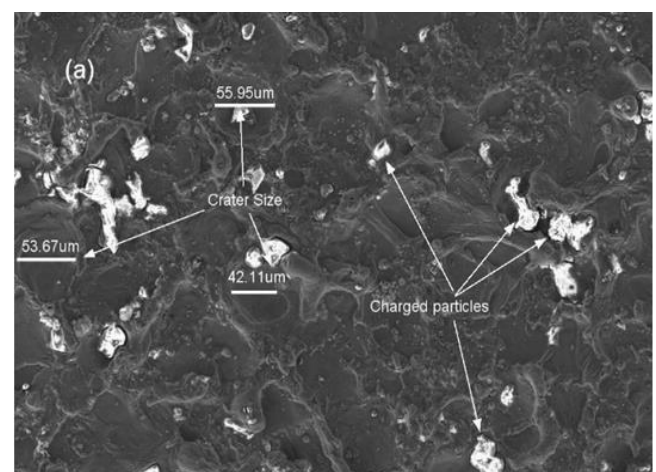


**Fig-7:** Experimental result (Brass) at I-5A, t<sub>on</sub> -14μs, Gap volt-50V

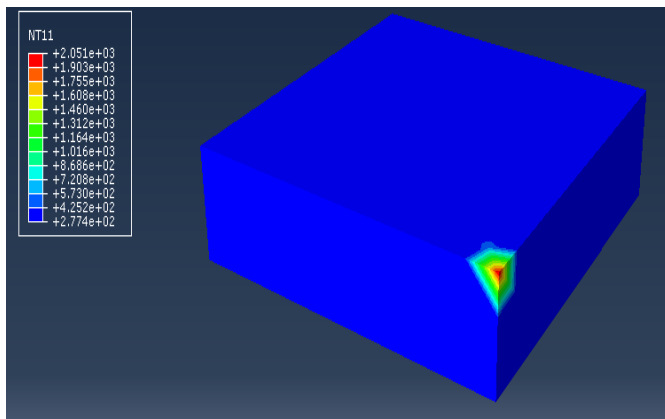


Fig.-8: Simulation result (Brass) at I-5A,  $t_{on}$ -14 $\mu$ s, Gap volt-50V

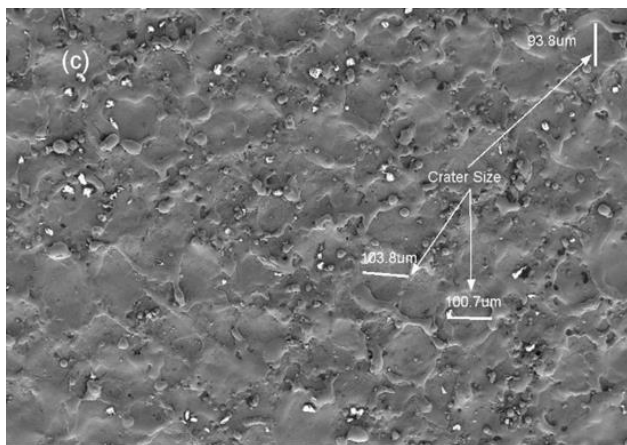


Fig.-9: Experimental result (Die steel D2) at I-5A,  $t_{on}$ -14 $\mu$ s, Gap volt-50V

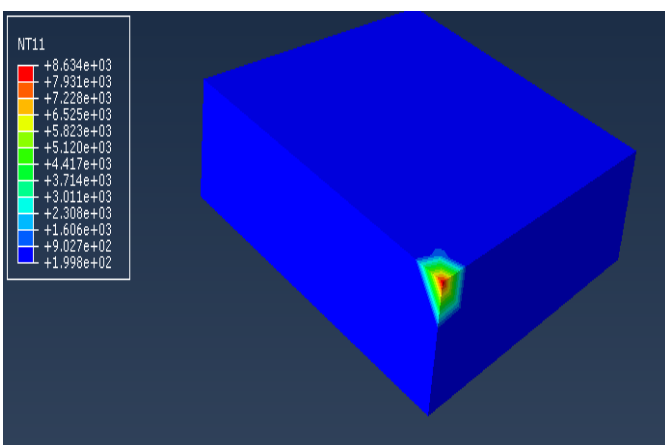


Fig.-10: Simulation result (Die steel D2) at I-5A,  $t_{on}$ -14 $\mu$ s, Gap volt-50V

Fig.5, fig.7 and fig.9 show the experimental result. Fig.6, fig.8 and fig.10 show the simulation result with experiment result at same parameter like current I 5, gap voltage 50V, discharge

time 14 $\mu$ s. From above simulation result we can consider that crater radius and crater depth do not depend upon only input parameter it also depend upon other factor like thermal materials properties. Simulated craters with various combinations of working parameters, the temperature circulation is obtained on the section following FE simulation.

The craters dimension is obtained in the model by removing the section element which is higher than the melting point at a temperature value. It can be found that the crater's radius in all simulations tends to be higher, giving an elliptical shape to the craters. This is because, due to the applied Gaussian heat flow at the top side, leading to more radial heat dissipation. In a heat-impaired area, the temperature gradients are below the crater surface.

### 5. VALIDATION OF RESULT

Condition taken in simulation is slightly different to the realistic condition like during machining there is no heat loss by radiation, no recast layer formed and no tool wear etc. So it is necessary validation of result with experimental result and simulation result to account error and find out the precise result.

$d_{ec}$  - Experimental crater radius

$h_{ec}$  - experimental crater depth

$d_s$  - Simulation crater radius

$h_s$  - Simulation crater depth

Table-3: ALMUNIUM simulation validation with experimental result.

Input parameter			Experimental result		Simulation result		Comparison with result			
$t_{on}$	I	VOLT	$d_{ec}$	$h_{ec}$	$d_s$	$h_s$	$d_{ec}/h_{ec}$	$d_s/h_s$	Error $d_s-d_{ec}$	Error $h_s-h_{ec}$
$\mu$ s	A	V	$\mu$ m	$\mu$ m	$\mu$ m	$\mu$ m				
14	5	50	49.3	29.0	54.9	31.7	1.70	1.73	5.56	2.697
			4	23	0	0				
20	8	50	58.8	37.9	65.4	43.5	1.55	1.50	6.67	5.55
			3	5	0	0				
25	10	50	67.3	49.8	75.8	54.5	1.37	1.29	8.47	5.63
			3	7	0	0		9		

**Table-4:** Brass simulation validation with experimental result.

Input parameter			Experimental result		Simulation result		Comparison with result			
$t_{on}$	I	VOL T	$d_{ec}$	$h_{ec}$	$d_s$	$h_s$	$d_{ec}/h_{ec}$	$d_s/h_s$	Error	Error
$\mu s$	A	V	$\mu m$	$\mu m$	$\mu m$	$\mu m$			$d_s-d_{ec}$	$d_s-h_{ec}$
14	5	50	25.30	15.33	30.50	18.50	1.65	1.685	5.2	3.17
20	8	50	29.32	19.54	34.60	23.10	1.50	1.4978	5.28	3.56
25	10	50	32.84	24.14	40.80	28.80	1.36	21.176	7.96	4.66

**Table-5:** Die steel d2 simulation validation with experimental result.

Input parameter			Experimental result		Simulation result		Comparison with result			
$t_{on}$	I	VOL T	$d_{ec}$	$h_{ec}$	$d_s$	$h_s$	$d_{ec}/h_{ec}$	$d_s/h_s$	Error	Error
$\mu s$	A	V	$\mu m$	$\mu m$	$\mu m$	$\mu m$			$d_s-d_{ec}$	$h_s-h_{ec}$
14	5	50	8.75	4.88	10.5	5.90	1.79	1.77	1.75	1.02
20	8	50	13.5	8.43	15.5	9.75	1.60	1.55	2	1.156
25	10	50	16.34	11.67	19.5	13.90	1.41	1.45	3.16	2.23

### 6. DISCUSSION

From above observation table 3, table 4 and table 5 it has observed that crater aspect ratio means ratio of crater radius and crater depth decreases with increases discharge current and discharge time. Due to increase discharge current and discharge time it causes increase heat flux distribution over time a period and discharge energy. During spark in machining zone, low energy causes less penetration of heat while high discharge energy causes depth penetration with heat. So crater aspect ratio decreases with increase in discharge energy. Also the dimensions of craters radius and craters depth are dependent upon the discharge energy as well as thermal material properties.

### 3. CONCLUSIONS

For the simulation of a single spark in EDM, a finite element model is proposed. The outstanding characteristics of this model include real assumptions such as with a distribution of Gaussian heat flux, discharge-on-time and current plasma channel range, temperature dependent material properties,

latent fusion heat, and a inconsistent cathode power and plasma flush efficiency. The results of this work are as follows:

1. From above result at same input parameter we consider that generation of crater profile is not only functioning of input parameter it also the function of temperature dependent materials property.
2. The radius of craters and depth of craters increase as operating parameter values such as pulse current and pulse on time increase. It is because the input pulses and the input heat flow time are increased.
3. At low discharge time and discharge current the craters aspect ratio displays a high values. This is because the radial heat distribution is significantly bigger at low operational parameters values.
4. A FEM model for single spark has been simulated with error 12.5% to 20% with realistic model and condition. As current research scenario error accounted during simulation is considerable.

### REFERENCES

- [1] Salah et al. After 60 years of EDM the discharge process remains still disputed. J Mater Process Techol 2004;149:376-81. doi:10.1016/j.jmatprotec.2003.11.060.
- [2] Shankar et al. Electro-thermal-based finite element simulation and experimental validation of material removal in static gap single- machining process. Proc Inst Mech Eng Part B J Eng Manuf 2017;231:28- 47. doi:10.1177/0954405415572661.
- [3] Marafona J. and Chousal J.A.G., "A finite element model of EDM based on the Joule effect" International Journal of Machine Tools & Manufacture, Volume 46, (2006):p.595-602.
- [4] Ahn and Chung, Son SM. Burr and shape distortion in micro-grooving of nonferrous metals using a diamond tool. KSME Int JOURNAL-ENGLISH Ed 2000;14:1244-9.
- [5] DiBitonto D, Eubank P, Patel MR, Barrufet M a. Theoretical models of the electrical discharge machining process. I. A simple cathode erosion model. J Appl Phys 1989;66:4095-103. doi:10.1063/1.343994.

- [6] Rebelo J.C., Dias A. Morao, Mesquita Ruy, Paulo Vassalo and Mario Santos, "An experimental study on electro-discharge machining and polishing of high strength copper-beryllium alloys" *Journal of Materials Processing Technology*, Volume 108, (2000):p.389-397.
- [7] Patel.M.R., Barrufet.M.A., Eubank.P.T. and DiBitonto.D.D, "Theoretical models of the electrical discharge machining process-II: the anode erosion model" *Journal of Applied Physics*, Volume 66, (1989):p. 4104-4111.
- [8] Yadav V, Jain VK, Dixit PM. Thermal stresses due to electrical discharge machining. *Int J Mach Tools Manuf* 2002;42:877-88. doi:10.1016/S0890-6955(02)00029-9.
- [9] Bhondwe et al.. Thermo-physical modeling of diesinking EDM process. *J Manuf Process* 2010;12:45-56. doi:10.1016/j.jmapro.2010.02.001.
- [10] Marafona et al. (2006) Theoretical models of the electrical discharge machining process. III. The variable mass, cylindrical plasma model. *J Appl Phys* 1993;73:7900.
- [11] Kansal et al. (2008)A contribution in EDM simulation field. *Int J Adv Manuf Technol* 2015;79:921- 35. doi:10.1007/s00170-015-6880-1.
- [12] Bhattacharya, A. Batish, G. Singh, V.K. Singla, Optimal parameter settings for rough and finish machining of die steels in powder-mixed EDM, *Int. J. Adv. Manuf.Technol.* 61 (2012) 537-548.
- [13] Izquierdo et al. (2009)M, Klocke F. EDM simulation: finite element-based calculation of deformation, microstructure and residual stresses. *J Mater Process Technol* 2003;142:434-51. doi:10.1016/S0924-0136(03)00624-1.

## AUTHORS



Mr. Nishant Mishra, M.Tech scholar, Department of Mechanical engineering,SSIPMT, Raipur (C.G).



Mr. Atul Chakrawarti, Associate Professor, Department of Mechanical Engineering, SSIPMT, Raipur (C.G).